



HAL
open science

Study and experimentation of a 6-dB attenuation low-pass NGD circuit

Rivo Randriatsiferana, Yajian Gan, Fayu Wan, Wenceslas Rahajandraibe,
Rémy Vauché, Nour Murad, Blaise Ravelo

► **To cite this version:**

Rivo Randriatsiferana, Yajian Gan, Fayu Wan, Wenceslas Rahajandraibe, Rémy Vauché, et al.. Study and experimentation of a 6-dB attenuation low-pass NGD circuit. *Analog Integrated Circuits and Signal Processing*, 2022, 110 (1), pp.105-114. 10.1007/s10470-021-01826-x . hal-03494714

HAL Id: hal-03494714

<https://hal.science/hal-03494714v1>

Submitted on 7 Mar 2022

HAL is a multi-disciplinary open access archive for the deposit and dissemination of scientific research documents, whether they are published or not. The documents may come from teaching and research institutions in France or abroad, or from public or private research centers.

L'archive ouverte pluridisciplinaire **HAL**, est destinée au dépôt et à la diffusion de documents scientifiques de niveau recherche, publiés ou non, émanant des établissements d'enseignement et de recherche français ou étrangers, des laboratoires publics ou privés.

Study and Experimentation of a 6dB Attenuation Low-Pass NGD Circuit

Rivo Randriatsiferana¹, Yajian Gan², Fayu Wan³, Wenceslas Rahajandraibe*², Rémy Vauché², Nour M. Murad¹ and Blaise Ravelo³

¹University of La Reunion, LE2P Lab, Saint Denis, Réunion Island, France

²Aix-Marseille University, CNRS, University of Toulon, IM2NP UMR7334, Marseille, France

³Nanjing University of Information Science & Technology (NUIST), Nanjing, Jiangsu 210044, China

Abstract

Because of its counterintuitive nature, the Negative Group Delay (NGD) remains as an uncommon and unfamiliar electronic function. For this reason, the design and analysis of NGD circuits is not well-known for most of electronic designers. This paper initiates a basic and easy to understand theory, in addition to a design methodology for the low-pass NGD function. The circuit theory on the low-pass NGD function is described using a NGD passive topology which is constituted by a RC-parallel network with a resistive load. The NGD analysis and synthesis equations in function of NGD specifications are provided and a proof-of-concept of 6dB low-pass NGD circuits has been designed, simulated, fabricated and tested. Frequency and time domain analyses have been performed to validate the low-pass NGD function. Theoretical and simulated results are in very good agreement and a NGD has been obtained in measurement for the proposed structure.

Keywords: Circuit theory, low-pass NGD function, negative group delay (NGD), NGD analysis, passive topology, time-domain measurement.

1. Introduction

The delay effects are susceptible to limit certain electronic, electrical and automatic system performances [1-7]. The control systems are literally dependent to the delay [1] and performances of network control systems with energy constraint can be degraded by delay [2]. The delay is modelled in electronic components such as CMOS circuits [3] and Printed Circuit Board (PCB) electrical interconnect since it is one of the main parameters affecting the signal integrity [4, 5]. In addition to the noise effects, the Group Delay (GD) remains an open problem degrading communication data [6, 7]. To overcome this issue, delay insensitive circuits using time sharing technique have been proposed in [8]. However, delay functions have been developed for certain electronic systems [9-14]. For example, by exploiting the GD, a channel blind identification was proposed in [9]. In addition, electronic devices with delay lines have been designed in [10, 11] and radio frequency filters [12], and amplifiers [13] based on the time delay function have been proposed too.

To face up the delay effect, a compensation technique using a negative group delay (NGD) function has been initiated in [15]. The principle of NGD compensation is illustrated in Fig. 1 by considering a delay function which delays of τ the t -time dependent input signal V_{in} . This delay can be reduced to zero using a NGD function introducing a delay equal to $-\tau$. The global cascaded system also generates an output V_{out} in phase to V_{in} . Moreover, NGD circuits have been proposed for bilateral gain compensation and broadband switch-less bi-directional

amplifier [16, 17]. To understand this NGD function, a brief state of the art is described in the following paragraph.

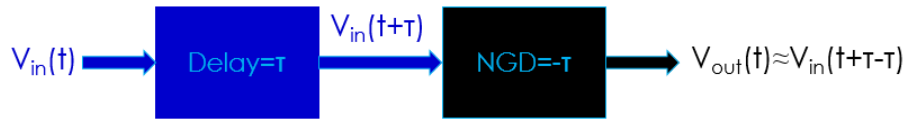


Figure 1. Delay compensation principle with NGD function.

The counterintuitive and unfamiliar NGD effect have been experimented with lumped electronic circuits since 1990s to 2010s [18-25]. Nevertheless, this intriguing effect which induces negative delay [18-22] remains unfamiliar for most of electronic designers because of its counterintuitive property to operate with output signals in time advance [20, 21] compared to input signals. This time-domain NGD effect is not in contradiction with the causality [18, 19] and for example the NGD effect has been experimented with audio signals [23]. Various NGD circuits based on lumped circuits have been designed [26-28]. But so far, despite the work done on this extraordinary function, the NGD function is still not clearly interpreted by non-specialist due to the circuit topology complexity [26-28]. Therefore, further studies are necessary for the understanding of this intriguing function as the common classical electronic functions such as filters, amplifiers, oscillators, phase shifters, etc. For this reason, a more general NGD theory has been initiated by considering the analogy with the linear filter behaviour [29-31].

The identification of Low-Pass (LP) and band-pass NGD functions built with lumped circuits have firstly been proposed in [29, 30]. For further understanding about the low-pass NGD concept, an NGD passive circuit operating with a 6dB attenuation is investigated in this paper which is organized in three main sections as follows. Section 2 theoretically investigates the LP NGD function and especially a LP NGD 6dB topology including its analysis, characterization and synthesis. Section 3 focuses on the results validation. Frequency domain analysis are firstly used to highlight the LP NGD behaviour. Then, time-domain simulations and experimentations are presented to verify the NGD function operation. Then, Section 4 concludes the paper.

2. Theory on the 6-dB NGD Circuit Under Investigation

The initiated circuit theory is aimed to indicate the basic element allowing to introduce the uncommon LP NGD function. Compared to the previous NGD papers published in literature, this paper focuses on the properties of a low-pass NGD passive circuit operating with a 6dB attenuation.

2.1 General specifications of LP NGD function

To be familiar with NGD systems, a simple and easy to understand representation is necessary. The present subsection addresses the theoretical approach related to the LP NGD circuit design.

2.1.1 Recall on the circuit and system parameter definitions

Figure 2 introduces a the LP NGD system having a Laplace transfer function $N(s)$ which links the input signal V_{in} to the output signal V_{out} in Laplace domain. As shown in the right part of

Fig. 2, the output signal can appear in advance in the time domain compared to the input signal thanks to the NGD function.

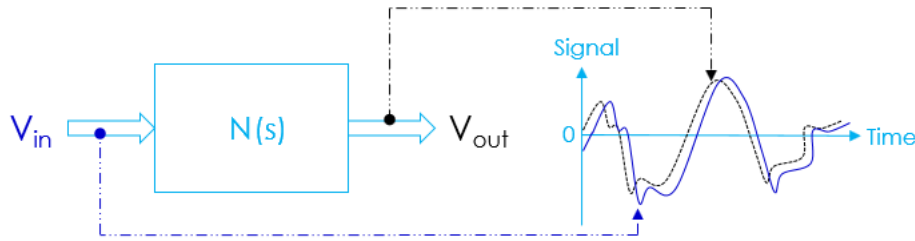


Figure 2. LP NGD system black box and behavior of transient input, and output signals.

Similar to classical engineering system, the analysis can be performed with the transfer function. Based on the classical circuit theory, by denoting the Laplace variable s , we can express the associated Voltage Transfer function (VTF) traditional defined as:

$$N(s) = \frac{V_{out}(s)}{V_{in}(s)}. \quad (1)$$

By denoting the angular frequency ω , the associated magnitude and phase can respectively be written as follows:

$$N(\omega) = |N(j\omega)| \quad (2)$$

$$\varphi(\omega) = \arg[N(j\omega)] \quad (3)$$

and the associated group delay (GD) is given by:

$$GD(\omega) = \frac{-\partial\varphi(\omega)}{\partial\omega}. \quad (4)$$

2.1.2 Guideline design of LP NGD circuit

Generally, the ideal frequency responses of LP NGD system can be represented as illustrated in Fig. 3. Figure 3(a) shows the ideal group delay (GD) response of a LP NGD function and Fig. 3(b) shows the ideal magnitude response. It is important to underline that the LP NGD should not be confused with the classical LP filter. Compared to usual system analysis, the NGD analysis focuses on the GD response but not the magnitude response. Thus, a LP NGD function is a system having a NGD for low frequencies. However, the NGD effect is obtained for low frequencies with passive circuits at the cost of an attenuation of N_0 in the NGD bandwidth BW_{NGD} . The main specifications of LP NGD function are also the GD value and the NGD cut-off frequency ω_n defined as follows:

$$GD_0 = GD(\omega \approx 0) < 0 \quad (5)$$

$$GD(\omega_n) = 0 \quad (6)$$

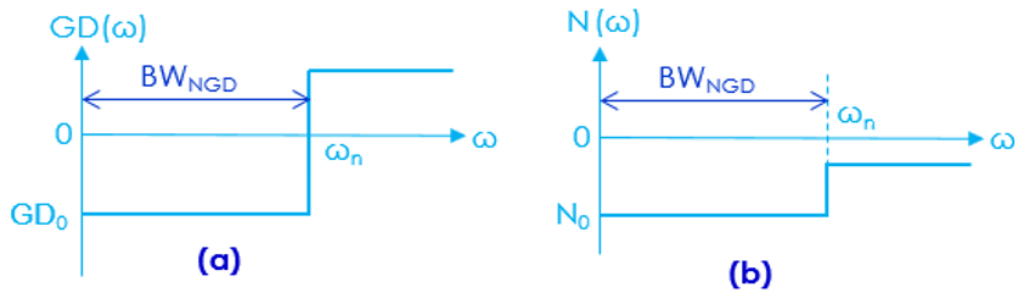


Figure 3. (a) GD and (b) magnitude ideal response of LP NGD function.

2.1.3 Recall on the circuit and system parameter definitions

Because of its counterintuitive effect, the NGD function remains so far as an unfamiliar electronic function. Therefore, an academic design method should be initiated to open the NGD engineering to non-specialists. Fig. 4 introduces the basic actions to be fulfilled during the design of a LP NGD circuit.

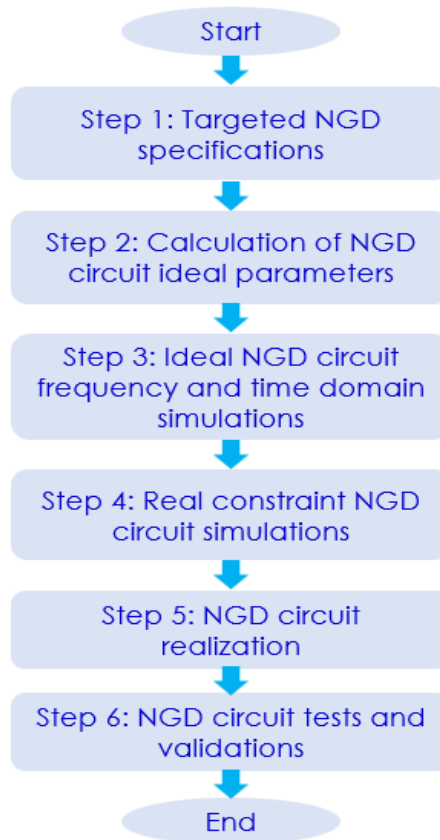


Figure 4. LP NGD circuit design flow.

2.2 Passive circuit-based LP NGD analysis

The LP NGD analysis consists in demonstrating the possibility to generate a GD with negative value in function of the circuit parameters.

2.2.1 NGD properties

Fig. 5 presents the simple investigated LP NGD circuit. Its passive topology consists of a RC-parallel network followed by a resistive load R . This circuit looks as a basic familiar passive cell but few investigations have been made to illustrate the possibility of generating LP NGD function from such a simple topology.

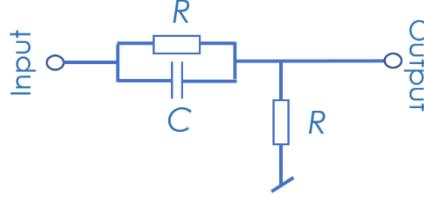


Figure 5. Passive circuit under study.

Considering the circuit shown in Fig. 5, the VTF introduced in (1) can be expressed as follows:

$$N(s) = \frac{R}{R + \frac{R}{1 + RCs}} \quad (7)$$

2.2.2 Analytical investigation on the NGD circuit frequency responses

After analytical calculation, it can easily demonstrate that this VTF can be expressed as the canonical form:

$$N(s) = \frac{1 + \tau s}{2 + \tau s} \quad (8)$$

with:

$$\tau = RC > 0 \quad (9)$$

Thus, the magnitude and phase frequency responses of the passive circuit can respectively be written as follows:

$$N(\omega) = |N(j\omega)| = \frac{\sqrt{1 + (\tau\omega)^2}}{\sqrt{4 + (\tau\omega)^2}} \quad (10)$$

$$\varphi(\omega) = \text{atan}(\tau\omega) - \text{atan}(\tau\omega/2) \quad (11)$$

The GD of the circuit shown in Figure 4 is given by:

$$GD(\omega) = \frac{\tau [(\tau\omega)^2 - 2]}{[1 + (\tau\omega)^2][4 + (\tau\omega)^2]} \quad (12)$$

2.3 NGD characteristics

The NGD characteristics depends on the specifications initially introduced in Fig. 3. The calculation of these characteristics as a function of the considered circuit parameters is proposed in this subsection.

2.3.1 Analysis of the 6-dB NGD circuit

From the VTF expressed in (8), the NGD analysis can be elaborated. The associated magnitude and GD at very low frequencies ($\omega \approx 0$) are given by:

$$N_0 = 1/2 \Leftrightarrow N_{0-dB} = -6 \text{ dB} \quad (13)$$

$$GD_0 = -\frac{\tau}{2} \quad (14)$$

It means that at very low frequencies, the RC-network presents a GD always negative for any parameters R and C. The LP NGD cut-off frequency, which is equal to the NGD bandwidth BW_{NGD} for a LP NGD circuit, can be expressed as follows:

$$\omega_n = \frac{\sqrt{2}}{\tau} \quad (15)$$

or

$$\omega_n = \frac{-1}{\sqrt{2GD_0}}. \quad (16)$$

2.3.2 NGD circuit design equations

The synthesis equation of this 6-dB LP NGD circuit aims to calculate the parameter R or C from the desired value of GD_0 equal to $\tau_n < 0$. By fixing for example the resistor value R, the capacitor can be computed from the equation:

$$C = \frac{-2 \cdot \tau_n}{R}. \quad (17)$$

Table 1 addresses the range of values of RC and considered GD parameters. Then, the abacuses of $C=f(R, \tau_n)$ displayed in Fig. 6(a) and $C=f(R, \omega_n)$ shown in Figure 6(b) indicate the value of calculated capacitor in function of desired:

- GD value τ_n supposed between -1 μ s to -10 ns,
- and available resistance R supposed between 100 Ω to 1 k Ω .

It can be underlined that the capacitor element varies from $C_{min}=20$ pF to $C_{max}=20$ nF for the considered resistor and GD.

	Resistor	GD₀	Capacitor
Min.	$R_{min}=100 \Omega$	$\tau_{n-min}=-1 \mu\text{s}$	$C_{min}=20 \text{ pF}$
Max.	$R_{max}=1 \text{ k}\Omega$	$\tau_{n-max}=-10 \text{ ns}$	$C_{max}=20 \text{ nF}$

Table 1. Resistor, NGD and capacitor range of values.

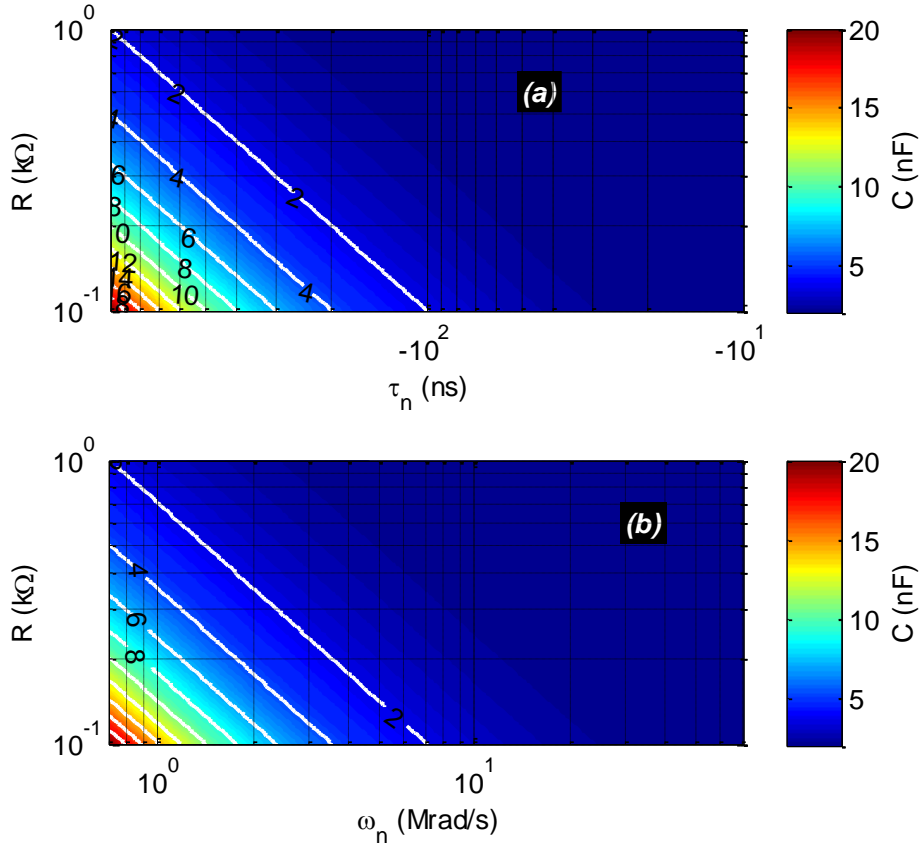


Figure 6. Abacuses of capacitor value versus (a) (R, τ_n) and (b) (R, ω_n) .

To verify the validity of the NGD theory, simulations and experimental investigations are discussed in the next section.

3. Validation Results

The present section introduces the validation of the 6-dB LP NGD function theorized in the previous section. The results are based on simulations run with the commercial tool ADS® electronic circuit design tool from Keysight Technologies® and measurements with discrete components soldered on a Printed Circuit Boards (PCBs).

3.1 Description of the 6-dB NGD circuit proof-of-concept

Following the NGD design flow introduced earlier in Fig. 4, a proof of concept circuit has been designed thanks to the theoretical analysis previously established. Accordingly, the LP 6-dB NGD circuit has been simulated in the ADS® schematic environment as displayed in Fig. 7(a) and a photograph of the fabricated prototype is shown in Fig. 7(b). This circuit has been implemented on a classical FR4 dielectric substrate presenting parameters given in Table 2. The PCB conductor traces have been obtained using copper.

Components	Description	Parameter	Value
Dielectric substrate	Material	FR4	-
	Relative permittivity	ϵ_r	4.5
	Loss tangent	$\tan(\delta)$	0.12
	Thickness	h	1.6 mm
Metallization	Material	Copper (Cu)	-
	Thickness	t	35 μm
	Conductivity	σ	58 MS/m

Table 2. Proof-of-concept circuit constituting material parameters.

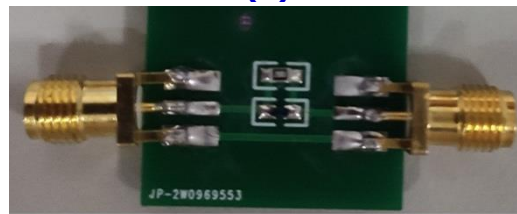
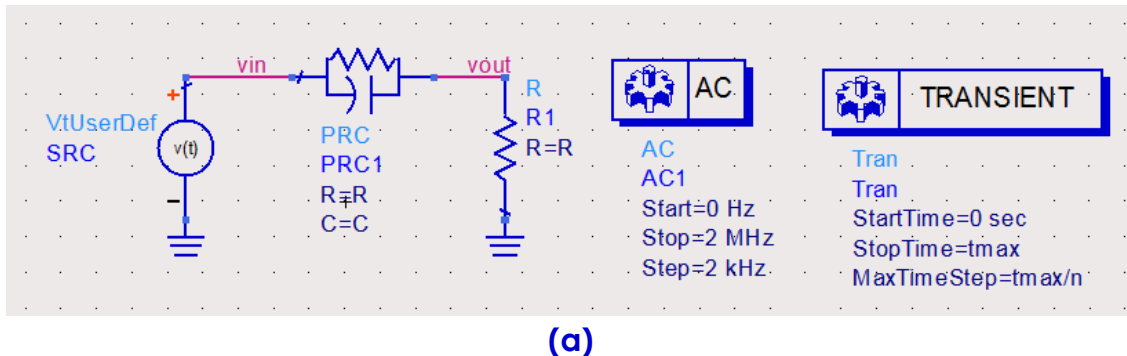


Figure 7. Schematic and photograph of LP NGD 6-dB prototype.

3.2 Discussion on results in frequency domain of the 6-dB LP NGD prototype

To perform the simulations, an NGD circuit have been designed to operate with a NGD value equal to $\tau_n = -0.3 \mu\text{s}$. The corresponding LP NGD circuit have been implemented with $R = 330 \Omega$ and $C = 1.82 \text{ nF}$. After AC simulations from DC to 2 MHz, frequency domain results have been plotted. Figure 8 presents the magnitude and the GD of the NGD circuit prototype. As expected, a LP NGD behavior is realized with $\text{GD} = -0.3 \mu\text{s}$ at very low frequencies. The magnitude and GD at very low frequencies confirms the 6dB LP NGD theoretical analysis. Moreover, the NGD cut-off frequency $f_n = \omega_n / (2\pi) = 375 \text{ kHz}$ agreed very well with equation (15).

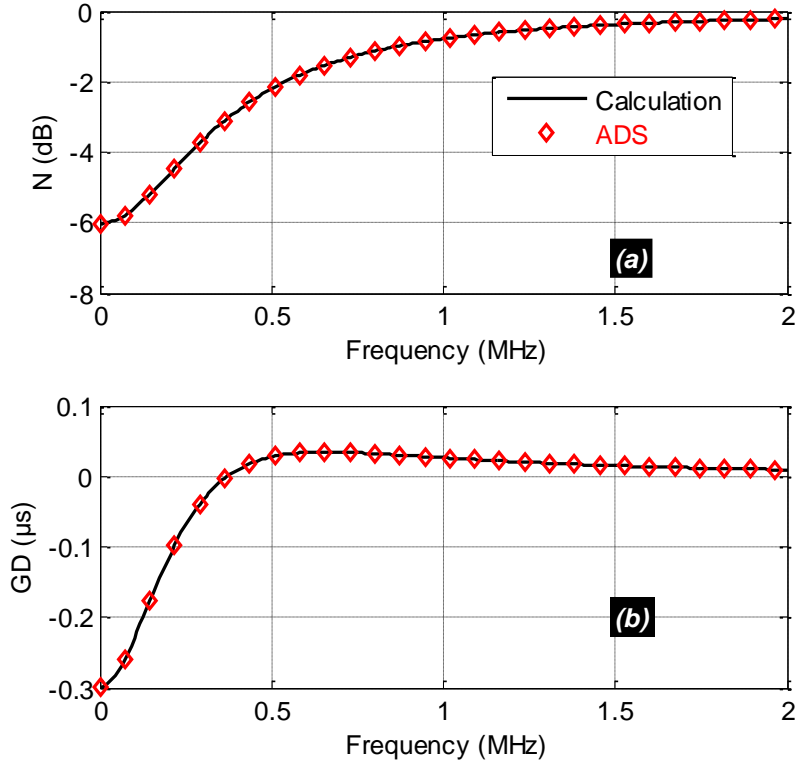


Figure 8. Frequency responses of the considered LP NGD circuit.

3.3 Discussion on time domain results of the 6-dB LP NGD prototype

Simulation and experimental investigations have been realized to validate the previously introduced theoretical analyses.

3.3.1 Simulated results

A typically arbitrary shape smoothed signal is necessary to demonstrate the LP NGD function in the potential applications. To realize the transient analysis, a sinc test input signal have been defined as in [32]:

$$v_{in}(t) = V_{max} \cdot \text{sinc}(2\pi \times t / T) \quad (17)$$

with $\text{sinc}(x) = \sin(x) / x$ which is equal to 1 when x is equal to 0. This signal was injected as input of the previously designed LP NGD circuit. The sinc pulse width has been set using $T = 2 \mu\text{s}$ and the amplitude V_{max} has been set to 1 V. Fig. 9(a) plots input signal and output signal, this last being obtained using analytical calculations and ADS® simulations. The calculated and simulated NGD outputs are in very good correlation. Fig. 9(b) shows normalized input and output signals in order to illustrate the time advance effect induced by the LP NGD function. It can be emphasized from this normalized plot that the output is in advance of about 0.3 μs . Moreover, the input and output signals present a very well-correlative behavior with negligible distortion when a sinc pulse is considered. It is noteworthy that the apparition of the signal advance depends on the matching between the NGD and input signal bandwidths. For further understanding on such matching, a cross correlation between the input and output versus the input signal bandwidth has been examined.

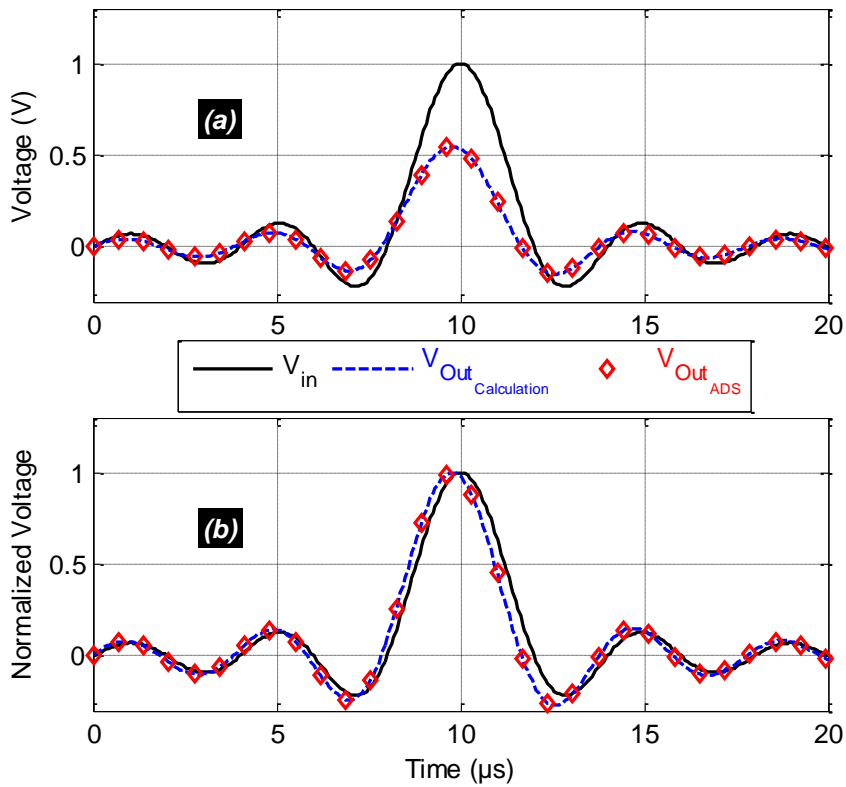


Figure 9. LP NGD POC transient simulation results.

It is very important to underline that the input and output present a very good integrity with almost negligible distortion despite the signal advance aspect. Table 3 indicates the cross correlation between the LP NGD circuit input and output versus the sinc pulse width.

T (μs)	1	2	3	5
x-correlation (%)	94.7	97.25	98.5	99.4

Table 3. Correlation Coefficient Between NGD Circuit Input and Output versus Sinc Pulse-width.

3.3.2 Measurement results

The configuration of the experimental setup is illustrated in Fig. 10. The time domain measurement has been settled in order to plot simultaneously the NGD circuit input and output signals, v_{in} and v_{out} , respectively. It has been realized with an arbitrary waveform signal generator and a digital oscilloscope as indicated in Table 4. The prototype of LP NGD circuit with 5% tolerances R and C components are designated in this table.

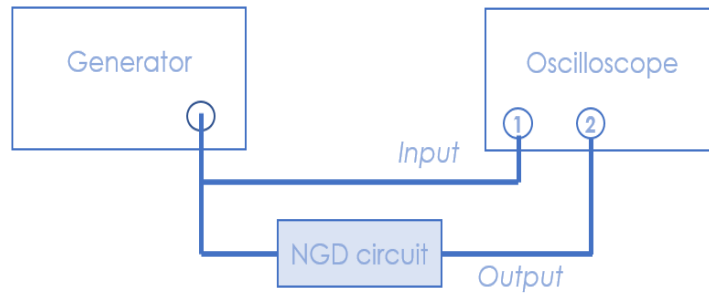


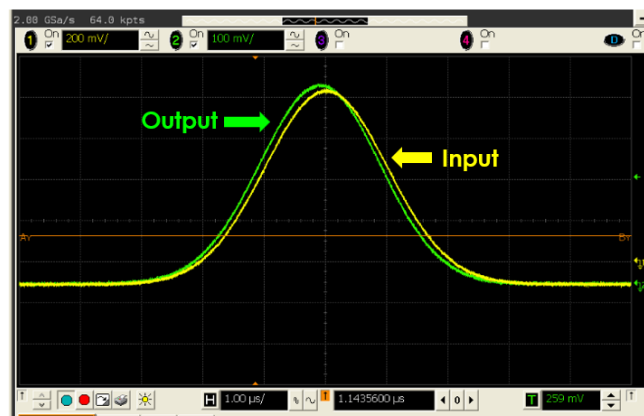
Figure 10. Experimental setup of NGD circuit time domain measurement.

Description	References	Parameters
Arbitrary function generator	Textronix AFG3102C DUAL CHANNEL	Sampling rate: 1 GS/s Bandwidth: 100 MHz
Digital oscilloscope	Agilent infiniiium MSO8104A	Sampling rate: 4 GS/s Bandwidth: 1 GHz
NGD circuit	Resistor	$R=470 \Omega$
	Capacitor	$C=0.56 \text{ nF}$

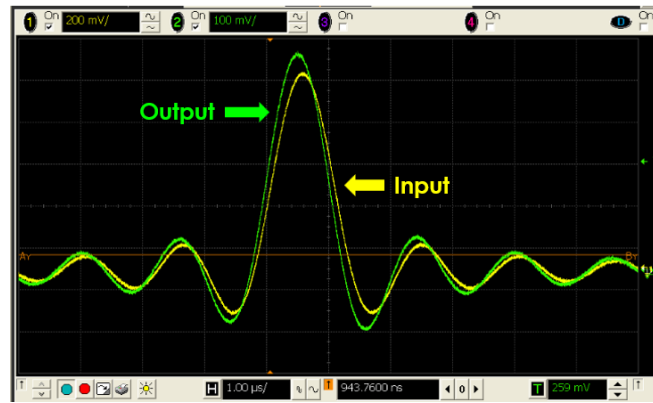
Table 4. Correlation coefficient between NGD circuit input and output versus sinc pulse-width.

The measurement results with different types of input test signals presenting amplitude $V_{max}=1 \text{ V}$ are displayed in Fig. 11. It is noteworthy that as predicted in previous simulations, normalized output signals are in advance compared to the input signals as illustrated in:

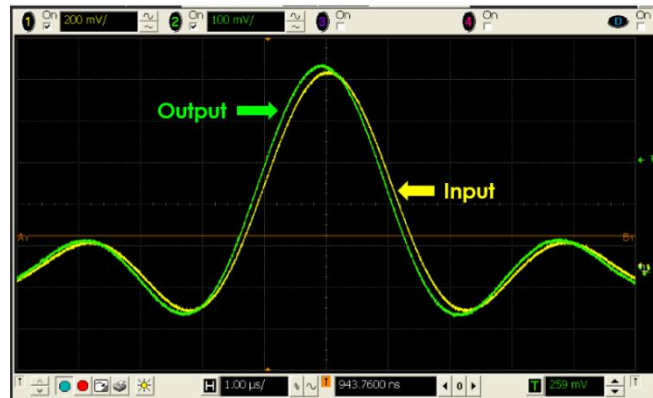
- Fig. 11(a) for a Gaussian input generated with a Pulse Repetition Frequency (PRF) of 50 kHz,
- Fig. 11(b) for a Sinc input generated with a PRF of 20 kHz and,
- Fig. 11(c) for a Sinc input generated with a PRF of 10 kHz.



(a)



(b)



(c)

Figure 11. Transient measurement results with: (a) Gaussian input pulse having a PRF equal to 50 kHz, (b) sinc input pulse having a PRF equal to 20 kHz and (c) sinc input pulse having a PRF equal to 10 kHz .

4. Conclusion

The basic theory allowing to understand and to be familiar to the NGD function has been established. The NGD design method and analyses have been performed on an innovative LP NGD passive function. The investigations demonstrate the possibility to obtain a NGD at the cost of a 6-dB attenuation only. The feasibility of the theory has been illustrated with the help of a commercial tool simulation and experimental validations, these ones being obtained using a prototype built with discrete passive component soldered on a PCB.

5. Acknowledgement

This research work was supported in part by NSFC under Grant 61971230 and 61601233, and in part by Jiangsu Distinguished Professor program and Six Major Talents Summit of Jiangsu Province (2019-DZXX-022), and in part by the Postgraduate Research & Practice Innovation Program of Jiangsu Province under Grant SJKY19_0974, and in part by the Priority Academic Program Development of Jiangsu Higher Education Institutions (PAPD) fund.

6. References

- [1] V. C. Pal and R. Negi, "Delay-Dependent Stability Analysis of Discrete Time Delay Systems with Actuator Saturation," *Transactions of the Institute of Measurement and Control*, vol. 40, no. 6, 2017, pp. 1873–1891. DOI: <https://doi.org/10.4236/ica.2012.31005>
- [2] J.-W. Hu, X.-S. Zhan, J. Wu, and H.-C. Yan, "Optimal Tracking Performance of NCSs with Time-delay and Encoding-decoding Constraints," *International Journal of Control, Automation, and Systems*, vol. 18, no. 4, pp. 1012-1022, Apr. 2020. DOI: <https://doi.org/10.1007/s12555-019-0300-5>
- [3] M-E. Hwang, S-O. Jung and K. Roy, "Slope Interconnect Effort: Gate-Interconnect Interdependent Delay Modeling for Early CMOS Circuit Simulation," *IEEE Transactions on Circuits and Systems I: Regular Papers*, vol. 56, no. 7, Jul. 2009, pp. 1428-1441. DOI: <https://doi.org/10.1109/TCSI.2008.2006217>
- [4] S.-M. Kang and H. Y. Chen, "A global delay model for domino cmos circuits with application to transistor sizing," *International Journal of Circuit Theory and Applications*, vol. 18, no. 3, pp. 289-306, May/June 1990. DOI: <https://doi.org/10.1002/cta.4490180306>
- [5] B. Ravelo, "Delay Modelling of High-Speed Distributed Interconnect for the Signal Integrity Prediction," *Eur. Phys. J. Appl. Phys.*, vol. 57 (31002), Feb. 2012, pp. 1-8. DOI: <https://doi.org/10.1051/epjap/2012110374>
- [6] G. Groenewold, "Noise and Group Delay in Active Filters," *IEEE Transactions on Circuits and Systems I: Regular Papers*, vol. 54, no. 7, July 2007, pp. 1471-1480. DOI: <https://doi.org/10.1109/TCSI.2007.900181>
- [7] S.-S. Myoung, B.-S. Kwon, Y.-H. Kim and J.-G. Yook, "Effect of Group Delay in RF BPF on Impulse Radio Systems," *IEICE Tran. Communications*, vol. 90, no. 12, 2007, pp. 3514-3522.
- [8] H. F. Li, S. C. Leung and P. N. Lam, "Optimised Synthesis of Delay-Insensitive Circuits Using Time-Sharing," *IEE Proceedings - Computers and Digital Techniques*, vol. 141, no. 2, Mar. 1994, pp. 111-118. DOI: <https://doi.org/10.1049/ip-cdt:19941001>
- [9] S. V. Narasimhan, M. Hazarathaiyah and P. V. S. Giridhar, "Channel Blind Identification Based on Cyclostationarity and Group Delay," *Signal Processing*, vol. 85, no. 7, July 2005, pp. 1275-1286. DOI: <https://doi.org/10.1016/j.sigpro.2005.01.011>
- [10] E. C. Heyde, "Theoretical Methodology for Describing Active and Passive Recirculating Delay Line Systems," *Electronics Letters*, vol. 31, no. 23, Nov. 1995, pp. 2038-2039. DOI: <https://doi.org/10.1049/el:19951356>
- [11] J. Vemagiri, A. Chamarti, M. Agarwal and K. Varahramyan, "Transmission Line Delay-Based Radio Frequency Identification (RFID) Tag," *Microwave and Optical Technology Letters*, vol. 49, no. 8, Aug. 2007, pp. 1900-1904. DOI: <https://doi.org/10.1002/mop.22599>
- [12] C. Wijenayake, Yongsheng Xu, A. Madanayake, L. Belostotski and L. T. Bruton, "RF Analog Beamforming Fan Filters Using CMOS All-Pass Time Delay Approximations," *IEEE Transactions on Circuits and Systems: Regular Papers*, vol. 59, no. 5, May 2012, pp. 1061-1073. DOI: <https://doi.org/10.1109/TCSI.2012.2185294>
- [13] L. N. Alves and R. L. Aguiar, "A time-delay technique to improve GBW on negative feedback amplifiers," *International Journal of Circuit Theory and Applications*, vol. 36, no. 4, June 2008, pp. 375-386. DOI: <https://doi.org/10.1002/cta.441>
- [14] R. S. Gau, J. Hsieh, and C. Lien, "Global exponential stability for uncertain bidirectional associative memory neural networks with multiple time-varying delays via LMI approach," *International Journal of Circuit Theory and Applications*, vol. 36, no. 4, June 2008, pp. 451-471. DOI: <https://doi.org/10.1002/cta.449>

- [15] B. Ravelo, "Recovery of Microwave-Digital Signal Integrity with NGD Circuits," *Photonics and Optoelectronics (P&O)*, vol. 2, no. 1, Jan. 2013, pp. 8-16. DOI: <https://doi.org/JPO10023>
- [16] M. Kandic and G. E. Bridges, "Bilateral Gain-Compensated Negative Group Delay Circuit," *IEEE Microwave and Wireless Components Letters*, vol. 21, no. 6, May 2011, pp. 308-310. DOI: <https://doi.org/10.1109/LMWC.2011.2132696>
- [17] Y. Meng, Z. Wang, S. Fang, T. Shao and H. Liu, "A Broadband Switch-Less Bi-Directional Amplifier with Negative-Group-Delay Matching Circuits," *Electronics*, vol. 7, no. 9, (158), 2018, pp. 1-11. DOI: <https://doi.org/10.3390/electronics7090158>
- [18] M. W. Mitchell and R.Y. Chiao, "Causality and Negative Group-delays in a Simple Bandpass Amplifier," *Am. J. Phys.*, vol. 66, 1998, pp. 14-19. DOI: <https://doi.org/10.1119/1.18813>
- [19] M. W. Mitchell and R. Y. Chiao, "Negative Group-delay and 'Fronts' in a Causal Systems: An Experiment with Very Low Frequency Bandpass Amplifiers," *Phys. Lett. A*, vol. 230, Jun. 1997, pp. 133-138. DOI: [https://doi.org/10.1016/S0375-9601\(97\)00244-2](https://doi.org/10.1016/S0375-9601(97)00244-2)
- [20] T. Nakanishi, K. Sugiyama and M. Kitano, "Demonstration of Negative Group-delays in a Simple Electronic Circuit," *Am. J. Phys.*, vol. 70, no. 11, 2002, pp. 1117-1121. DOI: <https://doi.org/10.1119/1.1503378>
- [21] M. Kitano, T. Nakanishi and K. Sugiyama, "Negative Group-delay and Superluminal Propagation: An Electronic Circuit Approach," *IEEE J. Sel. Top. in Quantum Electron.*, vol. 9, no. 1, Feb. 2003, pp. 43-51. DOI: <https://doi.org/10.1109/JSTQE.2002.807979>
- [22] J. N. Munday and R. H. Henderson, "Superluminal Time Advance of a Complex Audio Signal," *Appl. Phys. Lett.*, vol. 85, July 2004, pp. 503-504. DOI: <https://doi.org/10.1063/1.1773926>
- [23] W. Jian-Wu and F. Zheng-He, "Time-domain nature of group delay," *Chin. Phys. B*, vol. 24, no. 10 (100301), 2015, pp. 1-5. DOI: <https://iopscience.iop.org/article/10.1088/1674-1056/24/10/100301/meta>
- [24] F. Wan, J. Wang, B. Ravelo, J. Ge, and B. Li, "Time-Domain Experimentation of NGD Active RC-Network Cell," *IEEE Transactions on Circuits and Systems II: Express Briefs*, vol. 66, no. 4, Apr. 2019, pp. 562-566. DOI: <https://doi.org/10.1109/ACCESS.2019.2922422>
- [25] H. Mao, L. Ye and L.-G. Wang, "High fidelity of electric pulses in normal and anomalous cascaded electronic circuit systems," *Results in Physics*, vol. 13, no. 102348, pp. 1-9, June 2019. DOI: <https://doi.org/10.1016/j.rinp.2019.102348>
- [26] N. S. Bukhman and S. V. Bukhman, "On the Negative Delay Time of a Narrow-Band Signal as It Passes through the Resonant Filter of Absorption," *Radiophysics and Quantum Electronics*, vol. 47, no. 1, 2004, pp. 66-76. DOI: <https://doi.org/10.1023/B:RAQE.0000031672.70934.3a>
- [27] K.-P. Ahn, R. Ishikawa, A. Saitou and K. Honjo, "Synthesis for Negative Group Delay Circuits Using Distributed and Second-Order RC Circuit Configurations," *IEICE Trans. Electron.*, vol. E92.C, no. 9, 2009, pp. 1176-1181. DOI: <https://doi.org/10.1587/transele.E92.C.1176>
- [28] M. T. Abuelma'atti and Z. J. Khalifa, "A new CFOA-based negative group delay cascaded circuit," *Analog Integrated Circuits and Signal Processing*, vol. 95, pp. 351-355, Mar. 2018. DOI: <https://doi.org/10.1007/s10470-018-1172-y>
- [29] B. Ravelo, "Similitude between the NGD function and filter gain behaviours," *International Journal of Circuit Theory and Applications*, vol. 42, no. 10, Oct. 2014, pp. 1016-1032. DOI: <https://doi.org/10.1002/cta.1902>

- [30] B. Ravelo, "On the low-pass, high-pass, bandpass and stop-band NGD RF passive circuits," *URSI Radio Science Bulletin*, vol. 2017, no. 363, Dec. 2017, pp. 10-27. DOI: <https://doi.org/10.23919/URSIRSB.2017.8409424>
- [31] B. Ravelo, "First-order low-pass negative group delay passive topology," *Electronics Letters*, vol. 52, no. 2, Jan. 2016, pp. 124–126. DOI: <https://doi.org/10.1049/el.2015.2856>
- [32] [Online]. Available: <http://mathworld.wolfram.com/SincFunction.html>. [Accessed 01 Mar 2020]